Available online at www.sciencedirect.com

SciVerse ScienceDirect

journal homepage: www.elsevier.com/locate/he

Flame front structure and burning velocity of turbulent premixed CH_4/H_2/air flames

Meng Zhang [a], Jinhua Wang [a,*], Yongliang Xie [a], Wu Jin [a], Zhilong Wei [a], Zuohua Huang [a,*], Hideaki Kobayashi [b]

[a] State Key Laboratory of Multiphase Flow in Power Engineering, Xi'an Jiaotong University, Xi'an 710049, PR China
[b] Institute of Fluid Science, Tohoku University, Sendai, Miyagi 980-8577, Japan

ARTICLE INFO

Article history:
Received 18 March 2013
Received in revised form
8 May 2013
Accepted 10 May 2013
Available online 18 July 2013

Keywords:
Hydrogen addition
Flame front structure
Turbulent burning velocity
OH-PLIF

ABSTRACT

Flame front structure of turbulent premixed CH_4/H_2/air flames at various hydrogen fractions was investigated with OH-PLIF technique. A nozzle-type burner was used to achieve the stabilized turbulent premixed flames. Hot-wire anemometer measurement and OH-PLIF observation were performed to measure the turbulent flow and detect the instantaneous flame front structure, respectively. The hydrogen fractions of 0%, 5%, 10% and 20% were studied. Results show that the flame front structures of the turbulent premixed flames are wrinkled flame front with small scale convex and concave structures compared to that of the laminar-flame front. The wrinkle intensity of flame front is promoted with the increase of turbulence intensity as well as hydrogen fraction. Hydrogen addition promotes the flame intrinsic instability which leads to the active response of laminar flame to turbulence and results in the much more wrinkled flame front structure. The value of S_T/S_L increases monotonically with the increase of u'/S_L and hydrogen fraction. The increase of S_T/S_L with the increase of hydrogen fraction is mainly attributed to the diffusive-thermal instability effects represented by the effective Lewis number, Le_{eff}. A general correlation between S_T/S_L and u'/S_L is provided from the experimental data fitting in the form of $S_T/S_L \propto a(u'/S_L)^n$, and the exponent, n, gives the constant value of 0.35 for all conditions and at various hydrogen fractions.

1. Introduction

Natural gas is regarded as one of the most promising clean alternative fuels and has been widely used in industry, transportation and domestic appliance, such as gas turbine, boilers, internal combustion engines and residential cooking and heating. Methane, which is the main component of natural gas, has the unique tetrahedral molecular structure with high C–H bond energy, thus it demonstrates some unique combustion characteristics such as high ignition temperature and low flame propagation speed. Those will result in the slow burning velocity, poor lean-burn ability and high combustion instability for natural gas [1,2]. One effective method to solve these problems is to mix the natural gas with a fuel possessing high burning velocity. Hydrogen is the best candidate because of its low ignition energy, high reactivity, high diffusivity and subsequently high burning velocity. The laminar burning velocity of hydrogen is seven times to that of methane [3,4]. Meanwhile, hydrogen is a potentially clean alternative fuel to the fossil fuels in the future. Hydrogen is considered as a near

* Corresponding authors. Fax: +86 29 82668789.
E-mail addresses: jinhuawang@mail.xjtu.edu.cn (J. Wang), zhhuang@mail.xjtu.edu.cn (Z. Huang).
0360-3199/$ – see front matter
http://dx.doi.org/10.1016/j.ijhydene.2013.05.051

perfect energy carrier, which can be produced from fossil fuel and renewable energy such as solar power [5,6]. However, it is still far from the widespread use of pure hydrogen mainly due to the technical difficulties in terms of the storage, production and lack of the infrastructure [7]. Thus hydrogen enrichment hydrocarbons is the most promising bridge approach for the future hydrogen economy [6].

Previous works showed that a small fraction of hydrogen addition can significantly improve the thermal efficiency and decrease the emissions in spark-ignition internal combustion engine [8–11]. Studies on direct injection turbulent combustion showed that hydrogen addition can achieve the stable lean combustion along with low cyclic variations [12,13]. Experimental study on laminar premixed flames showed that the effect of hydrogen addition on the laminar burning velocity of CH_4/H_2/air mixtures is non-linear [14–16]. This suggests that hydrogen addition will significantly change the laminar-flame characteristics of CH_4/air mixtures. The turbulent combustion of CH_4/H_2/air has also been investigated experimentally by Fairweather et al. [17], Nakahara et al. [18], Schefer [19] and Strakey et al. [20]. A number of computational studies of lean premixed CH_4/H_2/air combustion system have focused on the flame response to local burning speeds [21], flame extinction and strained flows [20,22]. Results showed that there was clear increase in turbulence burning velocity for 20% H_2 for lean mixtures but not for rich. However, the previous experimental studies conducted in a combustion chamber and the flame propagation process in the combustion chamber is essentially transient. The turbulent premixed flame is essentially a random phenomenon. Thus, it is very difficult to investigate the flame front structure using combustion chamber. Meanwhile, the Burner stabilized Bunsen flame can provide continuous long duration measurement which is suitable for laser measurement and the subsequent flame front structure analysis. There were no investigations at lower hydrogen fraction (less than 10%) which is very important in combustor application. And the effect of hydrogen addition on the turbulence–flame interaction of hydrocarbons was still not well investigated and far from understood. This means that the mechanism of the hydrogen enrichment to improve the combustion characteristics of hydrocarbons/air is still not well understood and needs further study in details.

From the practical point of view, turbulent burning velocity is an important parameter for the design and optimization of combustion devices and the development of turbulent combustion models. A general correlation between turbulent burning velocity and parameters is essential. Thus, the measurement of turbulent burning velocity of CH_4/H_2/air mixtures is worth conducting.

The objective of the present study is to clarify the effects of hydrogen enrichment on turbulent burning velocity and the flame front structure of turbulent CH_4/air flames. Both turbulence measurements and OH detection by hot-wire anemometer and PLIF for the turbulent premixed flames were performed to describe the flow field and flame front structure. The laminar-flame characteristic parameters were calculated and the effects of hydrogen enrichment on flame–turbulence interaction were analyzed based on the scale of the laminar flame, the scale of the turbulence and the OH-PLIF flame front structures. A general correlation of turbulent burning velocities of CH_4/H_2/air mixtures was obtained based on the experimental results.

2. Experimental setup and procedures

Experiments were made using a nozzle-type turbulent premixed Bunsen burner with an outlet diameter of 20 mm by using OH-PLIF technique as shown in Fig. 1. The burner can achieve the stabilized turbulent premixed flames for OH-PLIF measurement, and it was sketched in Fig. 2. Turbulence is generated by a perforated plate installed 40 mm upstream of the nozzle outlet. Three kinds of plates were used to generate wide range of turbulence conditions. The orifice diameter and opening ratio are 2.1 mm, 3.5 mm, 4.0 mm, and 60%, 40%, 55%, respectively. The properties of the plates are shown in Fig. 3. A circular pilot flame slit with a thickness of 0.5 mm was designed at the nozzle outlet to support the flame stabilization for long duration OH-PLIF measurement. Hydrogen is

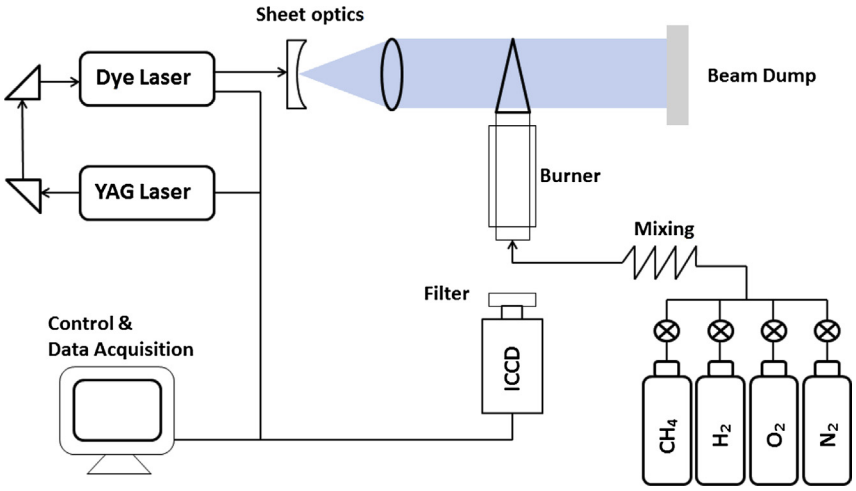

Fig. 1 – Schematic of the PLIF system.

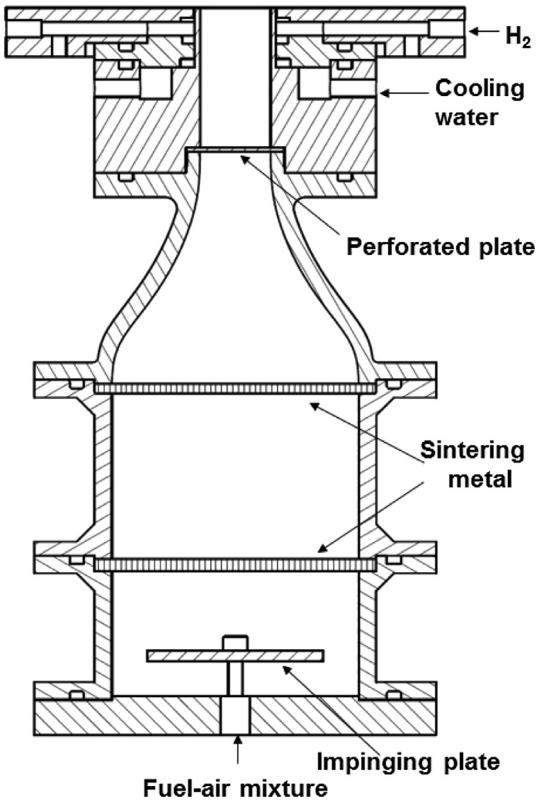

Fig. 2 – Schematic of the turbulent premixed Bunsen burner.

introduced to the circular slit to form a pilot flame which is used to ignite the main flame and support the flame stabilization. Cooling water with proper temperature can keep the burner nozzle stay away from high temperature and prevent water vapor condensation on the surface of nozzle. Two pieces of sintering metal with diameter of 100 μm are used to rectify the incoming flow and prevent flashback. An impinging plate is installed 10 mm down-stream of inlet to improve the mixing of the CH_4/H_2/air mixtures. The mean velocity at the nozzle outlet was controlled between about 2 m/s and 5 m/s to prevent the flashback and blowoff. Turbulence at the center and 10 mm above of the nozzle outlet was measured using a constant-temperature hot-wire anemometer (Dantec, Streamline 90N) and calculated assuming Taylor's hypothesis and isotropy of turbulence [23,24].

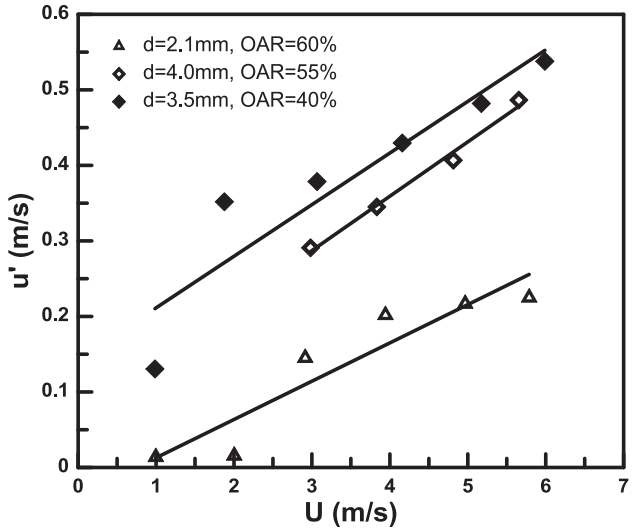

Fig. 3 – Properties of the perforated plates

Turbulent premixed flames of CH_4/H_2/air mixtures were stabilized at the nozzle burner outlet at normal pressure and temperature. The CH_4/H_2/air mixtures were premixed in a mixing bomb and supplied to the burner. Hydrogen fraction, ZH_2, is defined as $ZH_2 = XH_2/(XCH_4 + XH_2)$, where XH_2 and XCH_4 are the mole fractions of H_2 and CH_4, respectively. Four hydrogen fractions (0% H_2, 5% H_2, 10% H_2 and 20% H_2) were tested in the experiment. The laminar burning velocity, S_L, for the mixtures in this study was estimated by using the PREMIX code [25] and CHEMKIN-II database [26] with GRI-Mech 3.0 [27]. The laminar burning velocity is about 34 cm/s in this study. Equivalence ratio was adjusted to maintain the laminar burning velocity almost constantly at various hydrogen fractions. The properties of the mixtures were summarized in Table 1.

OH-PLIF measurements were performed to detect the instantaneous flame front structure of the turbulent premixed flames. The OH-PLIF measurement system consists of a laser source, which includes a Nd:YAG as pumping laser and a tunable dye laser, fluorescence detection using an ICCD camera (LaVision Image Prox), and the equipment for signal control and data acquisition. The schematic of the PLIF system was shown in Fig. 1. The frequency of laser pulse for LIF excitation is 10 Hz. A second harmonic Nd:YAG laser (Quanta-Ray Pro-190) with power of 300 mJ per pulse and pulse time of 10 ns. The baseline wavelength of the YAG laser is 1064 nm, and it is tuned to 355 nm by a harmonic generator with THG crystal arm. A pumped dye laser (SirahPRSC-G-3000) with a frequency doubler transfers the wavelength to 282.769 nm which is used to excite the Q1(8) line of the $A2\Sigma \leftarrow X2\Pi(1,0)$ transition with pulse energy of about 8 mJ. The laser goes through the energy monitor and sheet optics to produce a laser sheet of about 50 mm in height, and aligns to pass through the centerline of the burner nozzle. A $67 \times 50\ mm^2$ region was focused onto the monitor with resolution of 800*600 pixels. The OH fluorescence at wavelength around 308 nm was detected by an ICCD camera through a UV lens (Nikon Rayfact PF 10545MF-UV) with intensified Relay Optics (LavisionVC08-0094) and OH bandpass filter (LaVisionVZ08-0222). The ICCD camera locates perpendicularly with the laser sheet, and it operates with 200 ns gate width, 100 ns delay and 10 Hz image sampling frequency synchronized with laser.

Table 1 – The mixture properties in this study.

H_2 ratio	ϕ	S_L (cm/s)	T_b (K)	δ_L (mm)	L_M (mm)	ρ_b/ρ_u	Le_{eff}	l_i (mm)
0%	0.90	34.03	2133	0.066	0.25	0.141	0.96	1.36
5%	0.88	33.91	2111	0.067	0.24	0.141	0.86	1.14
10%	0.87	34.29	2100	0.067	0.24	0.144	0.79	0.98
20%	0.83	33.62	2051	0.071	0.23	0.148	0.68	0.74

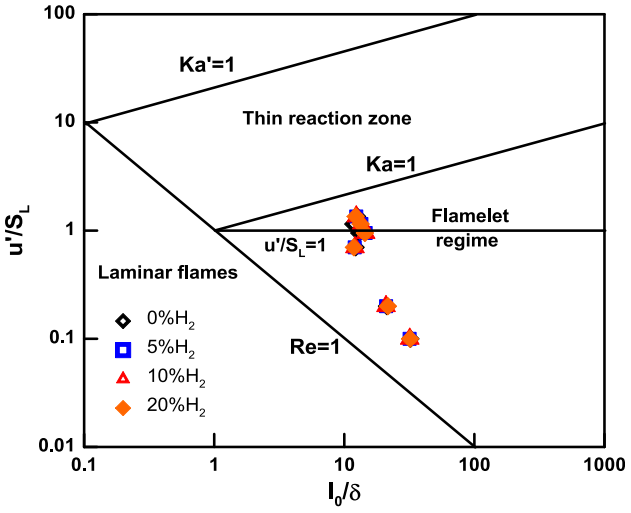

Fig. 4 – Borghi's diagram of turbulent premixed flames revised by Peters [30].

3. Results and discussion

3.1. *Effects of turbulence intensity and hydrogen addition on flame front structure*

It is well known that the characteristics of turbulent premixed flames quite depend on the regimes, the wrinkled laminar-flame regime, the distributed-reaction regime and the flamelets-in-eddies regime [28,29]. The three regimes are defined as $\delta_L \leq l_K$, $l_0 > \delta_L > l_K$ and $\delta_L > l_0$, respectively, where, δ_L, l_K, and l_0 are laminar-flame thickness, Kolmogorov microscale and turbulence macroscale (integral scale), respectively. The laminar-flame thickness was calculated by $\delta_L = \alpha_D/S_L$, where, α_D represents the thermal diffusivity of the unburned mixtures, S_L is the laminar burning velocity of the mixtures. Fig. 4 shows the turbulent premixed flames of the present work in the Borghi's diagram modified by Peters [30]. It can be seen that all the flames of the present work locate in the flamelet regime. Thus the flamelet model is applied in the following discussion.

Fig. 5 gives the direct images of the turbulent premixed CH_4/H_2/air flames. The flame brush of turbulent premixed flames is clearly demonstrated, however, the detailed information such as flame front structure can not be obtained because it is a projective image, and the exposure time is long to eliminate the high frequency random turbulent flame front information. The OH-PLIF images under the same experimental conditions of Fig. 5 are shown in Fig. 6. The wrinkled flame front can be well recognized using the OH-PLIF technique with high resolution and high sensitivity in this study. It is noted that all the flames in this study possess convoluted flame front structure with convex and concave cusps compared with the laminar-flame front which is a smooth shape, like triangle for the Bunsen flame [31] or spherical surface for the laminar-flame propagation [14]. Additionally, the flame front is more wrinkled with the increase of turbulence intensity. At low turbulence intensity, the scale of turbulent flow is larger and the flame front is wrinkled structure

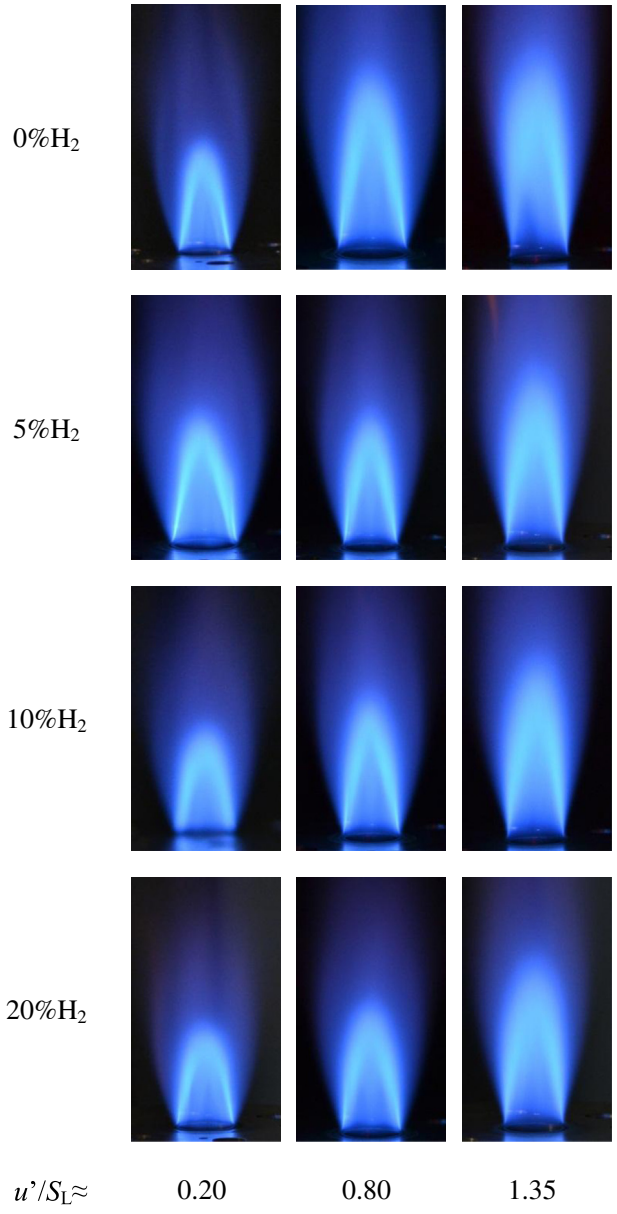

Fig. 5 – Direct images of the turbulent premixed flames of CH_4/H_2/air mixtures by a digital camera.

with large scale branches, because at this region the flame thickness is much smaller than the integral scale. Turbulent flow cannot access the inner part of the flame reaction region and the interaction between flow and flame is weak. With the increase of turbulence intensity, the flame front is more wrinkled and much finer due to the decrease of turbulent flow scale [32]. This reveals that the increase of turbulence intensity can decrease turbulence scale and further promote the flame front wrinkle intensity. With hydrogen addition, the flame front tends to be much finer and more wrinkled compared to that of CH_4/air flames under the same turbulence condition. This would be due to the effect of flame intrinsic instability which influences the flame–turbulence interaction. Table 1 gives the effective Lewis number, Le_{eff}, Markstein length, L_M, and the flame intrinsic instability scale, l_i, of the CH_4/H_2/air mixtures. Le_{eff} represents the diffusional–thermal

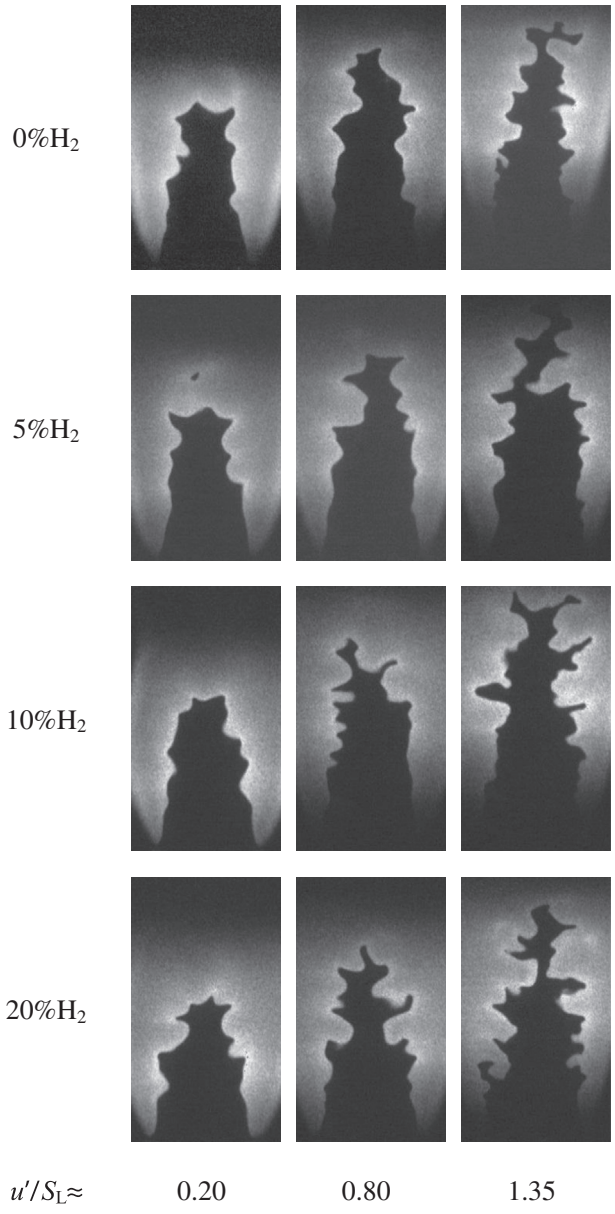

Fig. 6 – OH-PLIF images of turbulent premixed flames of CH_4/H_2/air mixtures.

instability [33,34] and it decreases from nearly unity for CH_4/air mixtures to much less than unity, for example, 0.68 for 20% hydrogen fraction. L_M correlates the local stretched burning velocity and unstretched burning velocity of the laminar

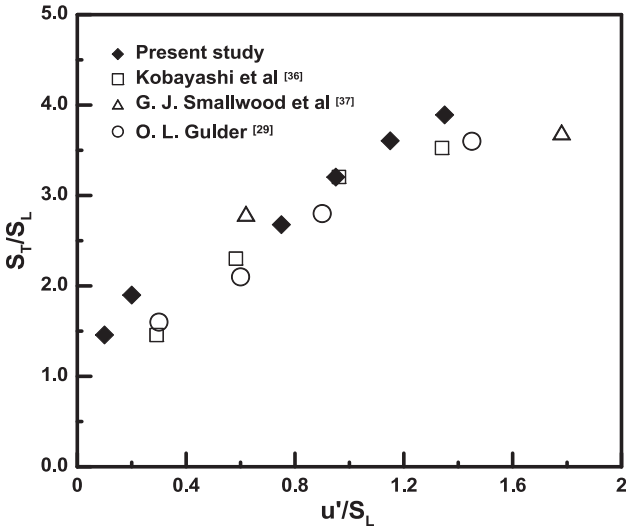

Fig. 8 – Comparison of turbulent burning velocity with previous studies.

flame. l_i is the characteristic scale of hydrodynamic combined with diffusive-thermal effects, which is calculated using nonlinear growth for sub-unity Lewis number [35]. It corresponds to the wavelength at the maximum growth rate of the dispersion relation of flame instability. l_i decreases significantly with the increase of hydrogen fraction. This indicates that the promotion of the flame intrinsic instability with hydrogen addition will lead to the active response of the flame to turbulence wrinkle and result in much finer and wrinkled flame front structure. It can also be noted that flame height tends to be higher with the increase of u'/S_L while flame height tends to be lower with the increase of hydrogen fraction caused by the increase of turbulent burning velocity with hydrogen addition. This will be discussed in the later section.

3.2. *Turbulent burning velocity of CH_4/H_2/air mixtures*

Fig. 7 gives the representative average of the single shot OH-PLIF images. Since the flame front structures of turbulent premixed flames are random, the statistical analysis is used to interpret the phenomenon. The average of 1, 50, 100, 300 and 500 pieces of OH-PLIF images are given. It is seen that the positions of the reaction zones move rapidly in space and produce a time-averaged view that reflects the appearance of the thick reaction zone. About 500 OH-PLIF images are sufficient to get the mean flame front location. Since OH radical

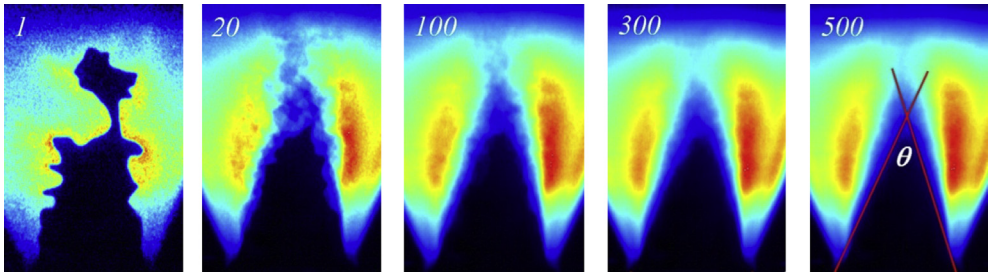

Fig. 7 – OH-PLIF images average and determine the mean flame cone.

concentration increased quickly at the flame front, the inner surface of this apparently thick reaction zone can be viewed as the averaged inner flame front of the turbulent premixed flames as the last image of Fig. 7 shown. The turbulent burning velocity, S_T, is obtained with conventional angle method [36] for the inner flame front, as

$$S_T = U \sin(\theta/2) \quad (1)$$

where θ is the inner flame front cone angle, U is the mean velocity of the mixture at burner exit.

The turbulent burning velocities of CH_4/air mixtures obtained in the study are compared with those of previous studies [29,36,37], as shown in Fig. 8. It is seen that all those data show a reasonable agreement within the experimental range. The relationship between turbulence intensity, u', and Kolmogorov scale, l_K, turbulence Reynolds number based on Taylor microscale, Re_λ, are given in Fig. 9. The Reynolds number increases almost linearly with turbulence intensity, u', while, Kolmogorov scale, l_K, decreases with u'. Furthermore, l_K, decreases rapidly when the turbulence intensity is low and the trend is significantly weakened at higher turbulence intensity. This reflects the fact that the turbulent flow changes apparently with turbulence intensity under weak turbulence condition.

Fig. 10 gives the variations of turbulent burning velocity, S_T, with the turbulence intensity, u', and turbulence Reynolds number, Re_λ. S_T increases almost linearly with the increase of u' and Re_λ for both CH_4/air and CH_4/H_2/air mixtures. S_T is higher for the mixtures with higher hydrogen fraction under all conditions in the experimental range, even though both mixtures have the same laminar burning velocity. The turbulent premixed flames of the present study locate on the flamelet regime. The increase of turbulent burning velocity in the flamelet regime is mainly due to not only the increase of flame front area caused by the turbulence wrinkle but also the increased local laminar burning velocity caused by the stretch effect. This means that the flame front area increases with the increase of hydrogen fraction caused by the enhanced wrinkled flame front. The diffusive-thermal instability represented by effective Lewis number, Le_{eff}, and intrinsic instability scale, l_i, given in Table 1 may be the reason for the increase of flame front area. On the other hand, local burning velocity S_{Lk} can be connected with S_L by (2).

$$S_L - S_{Lk} = L_M \alpha \quad (2)$$

where α is stretch rate and L_M represents Markstein length as shown in Table 1. It slightly decreased with hydrogen ratio and agreed well with the previous research [14]. This means that local stretched laminar burning velocities of all mixtures in this study were slightly smaller than S_L and the increase of flame front area was dominant factor for the increase of S_T/S_L. Moreover, only 5% hydrogen addition can lead to obvious difference to that of CH_4/air mixture. This suggests that hydrogen addition can significantly influence the flame characteristics and turbulence–flame interaction. In addition, turbulence Reynolds number based on Taylor microscale is an proper dimensionless parameter for turbulent combustion since S_T presents the similar trend with Re_λ as S_T with u' [38].

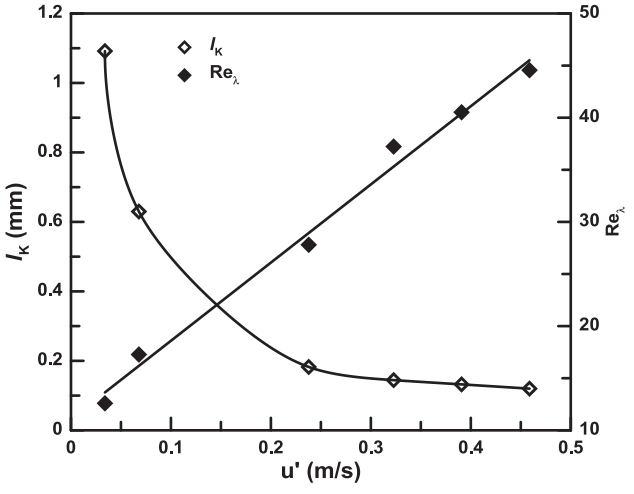

Fig. 9 – Relationship between turbulence parameters and mean outlet velocity. u' is turbulence intensity, l_k is Kolmogorov scale and Re_λ is turbulence Reynolds number.

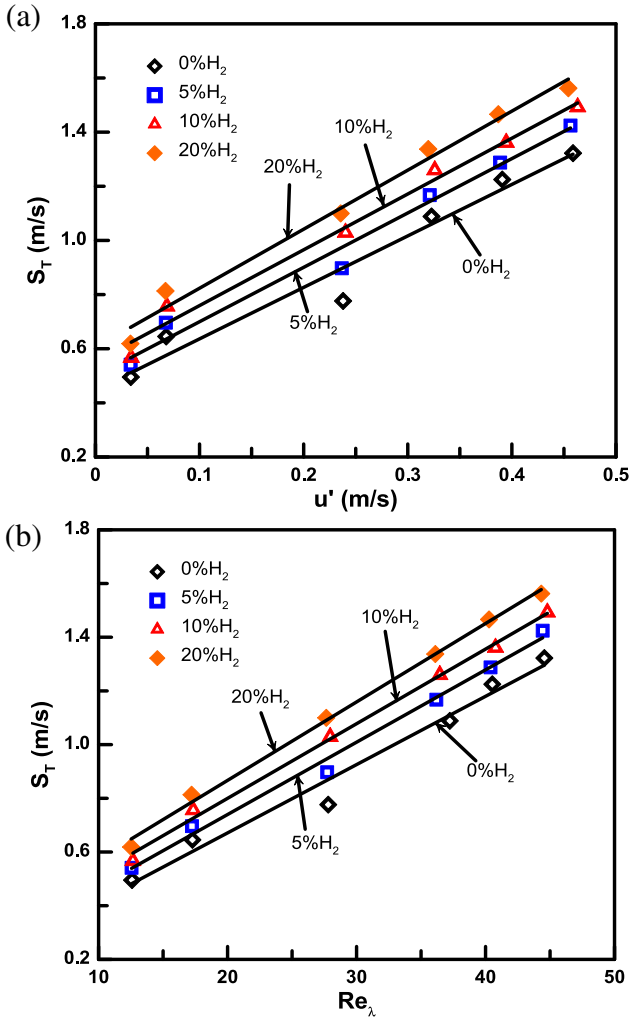

Fig. 10 – Variation of turbulent burning velocity with turbulence parameters: (a) S_T versus u'; (b) S_T versus Re_λ.

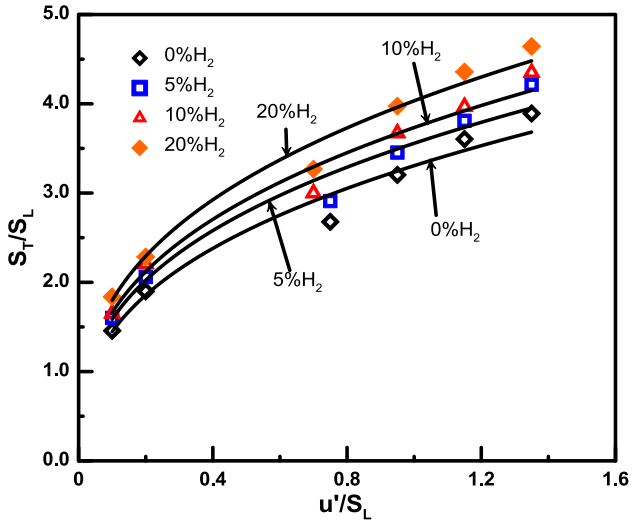

Fig. 11 – Variation of S_T/S_L with u'/S_L for CH_4/H_2/air mixtures.

3.3. *Correlation of turbulent burning velocities*

The relationship of S_T/S_L and u'/S_L was usually employed at turbulent combustion in previous researches [29,37]. u'/S_L indicates the information about turbulent flow and laminar flame, while, S_T/S_L indicates the information about turbulent flame and laminar flame. Fig. 11 gives the variation of S_T/S_L with u'/S_L. S_T/S_L increases monotonically with the increase of u'/S_L. Meanwhile, S_T/S_L increases with the increase of hydrogen fraction at the same u'/S_L.

Previous study proposed a general correlation of S_T/S_L as a power law function of the turbulence intensity (u'/S_L) [35,39].

$$S_T/S_L \propto a(u'/S_L)^n \quad (3)$$

In this study, a similar correlation is examined for the CH_4/H_2/airmixtures at various hydrogen fractions. The correlations of turbulent burning velocity for all mixtures are plotted in Fig. 12. The exponent n is about 0.35 under all experimental conditions in the study. This is consistent to the previous study on CH_4/air mixtures at high pressure that exponent n is close to 0.4 and remain almost constantly for the various mixtures [38,39]. The coefficient a is 3.3, 3.6, 3.7 and 4.0 which corresponds to the hydrogen fractions of 0%, 5%, 10% and 20%, respectively.

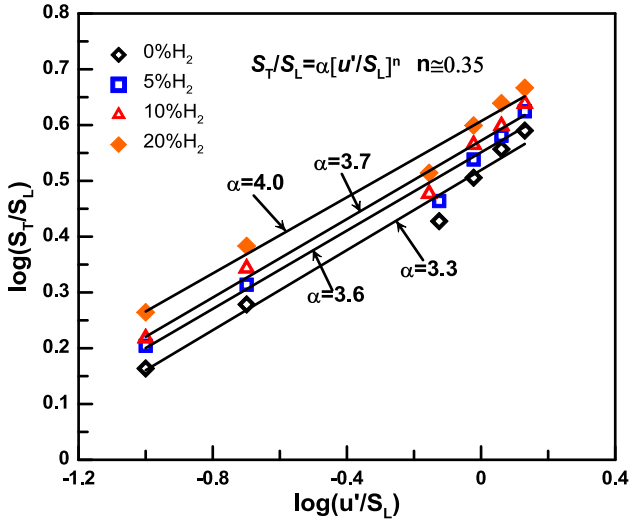

Fig. 12 – Correlation of turbulent burning velocities between S_T/S_L and u'/S_L for CH_4/H_2/air mixtures.

4. Conclusions

Flame front structure and turbulent burning velocity of CH_4/H_2/air mixtures at various hydrogen fractions were investigated with OH-PLIF technique. The effects of hydrogen addition and turbulence intensity on turbulence–flame interaction were analyzed based on the scale of laminar flame, the scale of turbulence and the OH-PLIF flame front structures. Main results are summarized as follows:

1. The flame front structures of turbulent premixed flames are the wrinkled flame front with small scale convex and concave structures compared to that of laminar flames. The wrinkle intensity of flame front is promoted with the increase of turbulence intensity as well as hydrogen fraction.
2. Hydrogen addition promotes the flame intrinsic instability which leads to the active response of laminar flame to turbulence and results in the much more wrinkled flame front structure.
3. S_T/S_L increases with the increase of hydrogen fraction which is attributed to the diffusive-thermal instability effects represented by effective Lewis number.
4. A general correlation between S_T/S_L and u'/S_L is provided from the experimental data fitting in the form of $S_T/S_L \propto a(u'/S_L)^n$. The exponent, n, gives a constant value of 0.35 under all conditions and at various hydrogen fractions.

Acknowledgments

This study is partially supported by National Natural Science Foundation of China (No. 51006080) and the Fundamental Research Funds for the Central Universities. Jinhua Wang acknowledges the Japan Society for the Promotion of Science for a JSPS Postdoctoral Fellowship grant.

REFERENCES

[1] Shrestha SOB, Karim GA. Hydrogen as an additive to methane for spark ignition engine applications. Int J Hydrogen Energy 1999;24:577–86.
[2] Turns SR. An introduction to combustion: concepts and applications. 2nd ed. Boston: McGraw-Hill; 2000. p. 158.
[3] Karim GA. Hydrogen as a spark ignition engine fuel. Int J Hydrogen Energy 2003;28:569–77.
[4] Bell SR, Gupta M. Extension of the lean operating limit for natural gas fueling of a spark ignited engine using hydrogen blending. Combust Sci Technol 1997;123:23–48.
[5] Zhang XR, Yamaguchi H, Cao YH. Hydrogen production from solar energy powered supercritical cycle using carbon dioxide. Int J Hydrogen Energy 2010;35:4925–32.

[6] Nowotny J, Sorrell CC, Sheppard LR, Bak T. Solar-hydrogen: environmentally safe fuel for the future. Int J Hydrogen Energy 2005;30:521–44.
[7] Petkov T, Veziroglu TN, Sheffield JW. An outlook of hydrogen as an automotive fuel. Int J Hydrogen Energy 1989;14:449–74.
[8] Hu EJ, Huang ZH, Liu B, Zheng JJ, Gu XL. Experimental study on combustion characteristics of a spark-ignition engine fueled with natural gas–hydrogen blends combining with EGR. Int J Hydrogen Energy 2009;34:1035–44.
[9] Wang JH, Huang ZH, Tang CL, Zheng JJ. Effect of hydrogen addition on early flame growth of lean burn natural gas–air mixtures. Int J Hydrogen Energy 2010;35:7246–52.
[10] Ma FH, Wang Y, Liu HQ, Li Y, Wang JJ, Zhao SL. Experimental study on thermal efficiency and emission characteristics of a lean burn hydrogen enriched natural gas engine. Int J Hydrogen Energy 2007;32:5067–75.
[11] Huang B, Hu EJ, Huang ZH, Zheng JJ, Liu B, Jiang DM. Cycle-by-cycle variations in a spark ignition engine fueled with natural gas–hydrogen blends combined with EGR. Int J Hydrogen Energy 2009;34:8405–14.
[12] Huang ZH, Wang JH, Liu B, Zeng K, Yu JR, Jiang DM. Combustion characteristics of a direct-injection engine fueled with natural gas–hydrogen blends under various injection timings. Energy Fuels 2006;20:1498–504.
[13] Wang JH, Huang ZH, Fang Y, Liu B, Zeng K, Miao HY, et al. Combustion behaviors of a direct-injection engine operating on various fractions of natural gas–hydrogen blends. Int J Hydrogen Energy 2007;32:3555–64.
[14] Hu EJ, Huang ZH, He JJ, Jin C, Zheng JJ. Experimental and numerical study on laminar burning characteristics of premixed methane–hydrogen–air flames. Int J Hydrogen Energy 2009;34:4876–88.
[15] Hu EJ, Huang ZH, Zheng JJ, Li QQ, He JJ. Numerical study on laminar burning velocity and NO formation of premixed methane–hydrogen–air flames. Int J Hydrogen Energy 2009;34:6545–57.
[16] Hu EJ, Huang ZH, He JJ, Miao HY. Experimental and numerical study on lean premixed methane–hydrogen–air flames at elevated pressures and temperatures. Int J Hydrogen Energy 2009;34:6951–60.
[17] Fairweather M, Ormsby MP, Sheppard CGW, Woolley R. Turbulent burning rates of methane and methane–hydrogen mixtures. Combust Flame 2009;156:780–90.
[18] Nakahara M, Shirasuna T, Hashimoto J. Experimental study on local flame properties of hydrogen added hydrocarbon premixed turbulent flames. J Therm Sci Technol 2009;4:190–201.
[19] Schefer R. Hydrogen enrichment for improved lean flame stability. Int J Hydrogen Energy 2003;28:1131–41.
[20] Strakey P, Sidwell T, Ontko J. Investigation of the effects of hydrogen addition on lean extinction in a swirl stabilized combustor. Proc Combust Inst 2007;31:3173–80.
[21] Vreman AW, van Oijen JA, de Goey LPH, Bastiaans RJM. Direct numerical simulation of hydrogen addition in turbulent premixed Bunsen flames using flamelet-generated manifold reduction. Int J Hydrogen Energy 2009;34:2778–88.
[22] Day MS, Gao X, Bell JB. Properties of lean turbulent methane–air flames with significant hydrogen addition. Proc Combust Inst 2011;33:1601–8.
[23] Kobayashi H, Kawahata T, Seyama K, Fujimari T, Kim JS. Relationship between the smallest scale of flame wrinkles and turbulence characteristics of high-pressure, high-temperature turbulent premixed flames. Proc Combust Inst 2002;29:1793–800.
[24] Kobayashi H, Nakashima T, Tamura T, Maruta K, Niioka T. Turbulence measurements and observations of turbulent premixed flames at elevated pressures up to 3.0 MPa. Combust Flame 1997;108:104–17.
[25] Kee RJ, Grcar JF, Smooke MD, Miller JA. A FORTRAN program for modeling steady, laminar, one-dimensional premixed flames. Report no. SNAD85-8240. Sandia National Laboratories; 1993.
[26] Kee RJ, Rupley FM, Miller JA. CHEMKIN II: a FORTRAN chemical kinetics package for the analysis of gas-phase chemical and plasma kinetics. Report no. SAND89-8009. Sandia National Laboratories; 1991.
[27] Gregory P, Smith DM, Frenklach Michael, Moriarty Nigel W, Eiteneer Boris, Goldenberg Mikhail, et al.; 1994.
[28] Turns SR. An introduction to combustion: concepts and applications. 2nd ed. Boston: McGraw-Hill; 2000. p. 450–75.
[29] Gülder ÖL. Turbulent premixed flame propagation models for different combustion regimes. Proc Combust Inst 1991;23:743–50.
[30] Peters N. Turbulent combustion. Cambridge UK: Cambridge University Press; 2000.
[31] Fu J, Tang CL, Jin W, Thi LD, Huang ZH, Zhang Y. Study on laminar flame speed and flame structure of syngas with varied compositions using OH-PLIF and spectrograph. Int J Hydrogen Energy 2013;38:1636–43.
[32] Murayama M, Takeno T. Fractal-like character of flamelets in turbulent premixed combustion. Proc Combust Inst 1989;22:551–9.
[33] Dinkelacker F, Manickam B, Muppala SPR. Modelling and simulation of lean premixed turbulent methane/hydrogen/air flames with an effective Lewis number approach. Combust Flame 2011;158:1742–9.
[34] Goix PJ, Shepherd IG. Lewis number effects on turbulent premixed flame structure. Combust Sci Technol 1993;91:191–206.
[35] Kobayashi H, Kawazoe H. Flame instability effects on the smallest wrinkling scale and burning velocity of high-pressure turbulent premixed flames. Proc Combust Inst 2000;28:375–82.
[36] Kobayashi H, Tamura T, Maruta K, Niioka T, Williams FA. Burning velocity of turbulent premixed flames in a high-pressure environment. Proc Combust Inst 1996;26:389–96.
[37] Smallwood GJ, Gülder ÖL, Snelling DR, Deschamps BM, Gökalp I. Characterization of flame front surfaces in turbulent premixed methane/air combustion. Combust Flame 1995;101:461–70.
[38] Kobayashi H, Seyama K, Hagiwara H, Ogami Y. Burning velocity correlation of methane/air turbulent premixed flames at high pressure and high temperature. Proc Combust Inst 2005;30:827–34.
[39] Kobayashi H, Kawabata Y, Maruta K. Experimental study on general correlation of turbulent burning velocity at high pressure. Proc Combust Inst 1998;27:941–8.